Surface Science 629 (2014) 15–19

Contents lists available at ScienceDirect

Surface Science

journal homepage: www.elsevier.com/locate/susc

Quantitation of enantiospecific adsorption on chiral nanoparticles from optical rotation

Nisha Shukla [a], Nathaniel Ondeck [b], Andrew J. Gellman [b,*]

[a] Institute for Complex Engineered Systems, Carnegie Mellon University, Pittsburgh, PA 15213, USA
[b] Department of Chemical Engineering, Carnegie Mellon University, Pittsburgh, PA 15213, USA

ARTICLE INFO

Available online 20 March 2014

Keywords:
Nanoparticles
Enantioselectivity
Chiral
Propylene oxide
Adsorption
Optical rotation

ABSTRACT

Au nanoparticles modified with enantiomerically pure D- or L-cysteine have been shown to serve as enantioselective adsorbents of R- and S-propylene oxide. A simple adsorption model and accompanying experimental protocol have been developed to enable optical rotation measurements to be analyzed for quantitative determination of the ratios of the enantiospecific adsorption equilibrium constants of chiral species on the surfaces of chiral nanoparticles, $K_L^S/K_D^S = K_D^R/K_L^R$. This analysis is robust in the sense that it obviates the need to measure the absolute surface area of the absorbent nanoparticles, a quantity that is somewhat difficult to obtain accurately. This analysis has been applied to optical rotation data obtained from solutions of R- and S-propylene oxide, in varying concentration ratios, with D- and L-cysteine coated Au nanoparticles, in varying concentration ratios.

1. Introduction

Over the course of the past decade, the field of nanoparticle (NP) synthesis has advanced rapidly to the point that it is now possible to control a wide variety of their physical, chemical and morphological characteristics: size, shape, composition, phases, etc. [1]. It is even possible to grow NPs with core–shell structures and other multiphase morphologies. The interest in controlled NP synthesis stems from the numerous important applications of NPs in catalysis, adsorption, pigments, and sensors. All of these applications can benefit from increased control of NP properties through control of their physical, chemical and morphological characteristics.

Nanoparticle chirality is a characteristic that has potential application in enantioselective chemical processes such as catalysis, adsorption and separations. Nanoparticle chirality has been known since the determination of the atomic structure of a Au_{102} NP coated with 44 *p*-mercaptobenzoic acid moieties revealed a symmetric fcc core surrounded by an asymmetric shell of Au atoms bound to the mercaptobenzoic acid ligands [2]. Since then, a number of such chiral NPs have been synthesized. For the most part, it is the chiro-optical properties of these NPs that have been explored rather than their enantiospecific interactions with chiral molecules [3–5]. However, it is the enantiospecificity of the adsorption energies and reaction barriers of chiral species on chiral surfaces that are the root origin of enantioselectivity in important chemical processes such as catalysis and separations [6,7]. Quantifying these remains a challenge.

There are a number of possible means for preparing chiral NPs in enantiomerically pure form [3,4,8–16]. The chiral NPs described above are synthesized from achiral reagents and the result is a racemic mixture of the NPs that needs to be separated enantioselectively. However, preparation of particles using enantiomerically pure chiral ligands will yield NPs with chiral surfaces. Most of the early syntheses of shape controlled NPs resulted in NPs that expose high symmetry low Miller index facets; however, in recent years there have been a number of examples of NPs that expose facets with high Miller index orientations such as (*hhl*). These have structures based on monoatomic steps separating atomically flat terraces. Although these are not naturally chiral planes [6,17–19], there is evidence from studies on bulk surfaces with these high Miller index orientations that they can be induced to reconstruct into naturally chiral planes with kinked step edges simply by adsorption of an appropriate chiral ligand [20–22]. Most recently, some NPs have been prepared to expose facets that are naturally chiral, however, they appear in equal distributions of both enantiomorphs around the NP. Given these various routes to the preparation of chiral NPs, the next step is to develop methods for detection, study and understanding of their enantiospecific interactions with chiral probe molecules.

In prior work, we used optical polarimetry to demonstrate that Au NPs coated with D- or L-cysteine (cys) adsorb chiral probes such as R- or S-propylene oxide (PO) enantioselectively [16]. During the addition of racemic PO to a solution containing D-cys/Au NPs, there is an increasing optical rotation by the solution with increasing concentration of rac-PO. With the addition of rac-PO to a solution containing L-cys/Au

* Corresponding author. Tel.: +1 412 268 3848.
E-mail address: gellman@cmu.edu (A.J. Gellman).

http://dx.doi.org/10.1016/j.susc.2014.03.011
0039-6028/

NPs, there is an increasing optical rotation but with opposite sign. Racemic PO itself does not rotate light in aqueous solution, nor does the addition of rac-PO to a solution containing rac-cys/Au. Therefore, the rotation of light by addition of rac-PO to a solution containing D-cys/Au (or L-cys/Au) NPs must arise from the enantioselective adsorption of one enantiomer of PO onto the chiral NPs and an enantioselective partitioning between the solution phase and the adsorbed phase. Furthermore, this is observable using optical polarimetry only because the enantiomer adsorbed on the Au NPs exhibits a specific optical rotation that is different from its specific optical rotation in solution phase. If the enantiomers in solution and in the adsorbed phase had identical intrinsic optical rotation constants, their enantiospecific partitioning between adsorbed and solution phases would not cause any change in the net optical rotation of the NP solution.

In addition to demonstrating the detection of enantioselective adsorption on chiral Au NPs using optical polarimetry, a simple adsorption model was proposed to analyze the optical rotation measurements to extract physical constants such as: the adsorption equilibrium constants, $K_D^R = K_L^S$ and $K_D^S = K_L^R$; the molar surface area of the NPs in solution, S_0; and the intrinsic optical rotation constants for the probe molecule in the adsorbed phase, α_{ads}^R and α_{ads}^S, and in the solution phase, α_{sol}^R and α_{sol}^S [16]. In this work, our analysis of that initial model shows that the equilibrium constants and the surface area are coupled to one another and cannot be determined independently unless the concentrations of PO are sufficiently high that the adsorption isotherms are no longer linear in the PO concentration. Although the PO concentrations did extend into the non-linear regime for those measurements; the uncertainty in the determination of each is probably higher than originally reported because of the coupling of K and S_0. One solution to this problem would be to find an independent means of determining S_0 that does not rely on the optical rotation data. However, the definition of S_0 is the effective molar surface area or concentration of PO adsorption sites on Au NP surfaces already modified by cysteine, not a quantity that can be measured readily.

In this work we propose and apply an analysis of optical rotation data that allows quantitative extraction of the enantiospecific ratios of the adsorption equilibrium constants, $K_L^S/K_D^S = K_D^R/K_L^R$, without the need to determine S_0. As it is the ratios of the adsorption equilibrium constants that determine the enantioselectivity of the adsorption process, they are as important as the absolute values of the equilibrium constants themselves. Obviating the need to measure S_0 is worth the sacrifice of the absolute values of the adsorption equilibrium constants.

2. Adsorption and optical rotation

The solutions on which we have made measurements of optical rotation contain both D- and L-cys/Au NPs and both R- and S-PO. The total concentrations of Au NPs and PO are fixed but the ratio of enantiomorphs varies from 100% of one to 100% of the other. To describe the enantiomeric excess of the PO in solution we define the quantity $\beta = 0 \rightarrow 1$ which quantifies the fractional concentration of R-PO in solutions also containing S-PO,

$$x_{tot}^{R-PO} = \beta \cdot x_{tot}^{PO} \tag{1}$$

$$x_{tot}^{S-PO} = (1-\beta) x_{tot}^{PO} \tag{2}$$

where x_{tot}^{PO} is the total PO concentration. Note that x_{tot}^{R-PO} includes both the R-PO in solution phase and adsorbed onto the Au NPs. To describe the enantiomeric excess of the cys/Au NPs in solution we define the quantity $\gamma = 0 \rightarrow 1$ which quantifies the fractional concentration of D-cys/Au in solutions that also contain L-cys/Au NPs,

$$x_{tot}^{D-cys/Au} = \gamma \cdot x_{tot}^{Au} \tag{3}$$

$$x_{tot}^{L-cys/Au} = (1-\gamma) x_{tot}^{Au} \tag{4}$$

where x_{tot}^{Au} is the total concentration of cys/Au NPs in solution.

The physical phenomena occurring in the solutions and that dictate the results of the polarimetry measurements are illustrated in Fig. 1. The four equilibria between the R-PO and S-PO in the solution phase and R-PO and S-PO adsorbed on the surfaces of the dissolved D-cys/Au and L-cys/Au NPs are characterized by four equilibrium constants. The quantity K_D^R is the equilibrium constant for adsorption of R-PO on D-cys/Au and has units of M^{-1}. The values of the four equilibrium constants are related by diastereomerism: $K_D^R = K_L^S \neq K_L^R = K_D^S$. The quantity S_0 represents the concentration in solution of the PO adsorption sites on the cys/Au NPs and has the units of M. In the context of a Langmuir isotherm the fractional coverage of adsorbed PO would be $\theta = 1$ when the concentration of PO in the adsorbed phase is equal to S_0; at that point, the cys/Au NP surfaces would be saturated with adsorbed PO. The quantities α are the specific optical rotation constants for PO in the solution phase, α_{sol}, and in the adsorbed phase, α_{ads}, and have the units (°/M). The specific optical rotation constants are related as follows: $\alpha_{ads}^R = -\alpha_{ads}^S \neq -\alpha_{sol}^S = \alpha_{sol}^R$. The key finding of our prior work that underpins the use of optical rotation for detection of enantiospecific adsorption in these systems is that $\alpha_{sol} \neq \alpha_{ads}$, thereby differentiating the optical properties such that the net optical rotation is dependent on the concentrations in the two phases [16].

We start with the Langmuir adsorption isotherm to describe the relationship between the concentration of R-PO in solution, $x_{sol}^{R/D}$, and the concentration in the adsorbed phase, $x_{ads}^{R/D}$, in the presence of D-cys/Au NPs. The concentration in solution of PO adsorption sites on the NPs is given by S_0.

$$\frac{x_{ads}^{R/D}}{S_0} = \frac{K_D^R x_{sol}^{R/D}}{1 + K_D^R x_{sol}^{R/D}} \approx K_D^R x_{sol}^{R/D} \tag{5}$$

$$x_{tot}^{R/D} = x_{sol}^{R/D} + x_{ads}^{R/D} \tag{6}$$

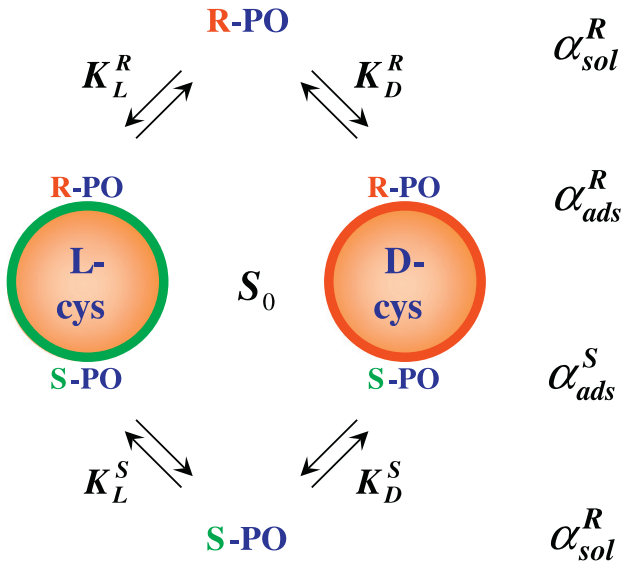

Fig. 1. Illustration of the physical phenomena and the physical constants that govern the optical rotation of solutions containing R- and S-PO with D- and L-cys/Au NPs. The equilibria between solution phase and adsorbed phase PO are determined by the equilibrium constants, K. The quantity, S_0, represents the concentration of PO adsorption sites on the cysteine modified Au NPs. The quantities α are the specific optical rotation constants for PO in the adsorbed and solution phases. Diastereomerism gives the following relationships between quantities: $K_D^R = K_L^S \neq K_L^R = K_D^S$, $\alpha_{ads}^R = -\alpha_{ads}^S$ and $\alpha_{sol}^R = -\alpha_{sol}^S$.

The approximation in Eq. (5) holds at low concentrations when the coverage in the adsorbed phase, $x_{ads}^{R/D}/S_0$, is linear in the solution phase concentration. In fact, for the purposes of this work the isotherm need not be Langmuirian; the only constraint on the isotherm is that it be linear at low concentrations. The concentrations of R-PO in solution, $x_{sol}^{R/D}$, and R-PO adsorbed on the D-cys/Au NPs, $x_{ads}^{R/D}$, are given in terms of the total concentration of R-PO, $x_{tot}^{R/D}$, by:

$$x_{sol}^{R/D} = \frac{x_{tot}^{R/D}}{1 + S_0 K_D^R} \tag{7}$$

$$x_{ads}^{R/D} = \frac{x_{tot}^{R/D} S_0 K_D^R}{1 + S_0 K_D^R}. \tag{8}$$

The rotation of polarized light by the addition of R-PO at a concentration $x_{tot}^{R/D}$ to a solution containing D-cys/Au NPs is then given by

$$\begin{aligned} \alpha_D^R\left(x_{tot}^{R/D}\right) &= \alpha_{sol}^R x_{sol}^{R/D} + \alpha_{ads}^R x_{ads}^{R/D} \\ &= \left(\frac{\alpha_{sol}^R + \alpha_{ads}^R S_0 K_D^R}{1 + S_0 K_D^R}\right) x_{tot}^{R/D}. \end{aligned} \tag{9}$$

Equivalent expressions describe the cases for the *S*/*D*, *R*/*L* and *S*/*L* combinations of PO and cys/Au NPs.

Two types of experimental protocols have been developed for extraction of the physical parameters determining optical rotation by R- and S-PO in solutions containing D- and L-cys/Au NPs. The first is one in which the concentration of D-cys/Au or L-cys/Au NPs is kept constant; their concentration is represented by S_0 in the formalism above. The total concentration of R- and S-PO is also held constant but the fraction of each as quantified by, β, is varied from 0 to 1. The optical rotation of light, $\alpha(\beta)$, is measured as a function of the fractional concentrations of R- and S-PO. Using the total concentration of PO, x_{tot}, and the independently measured value of the specific optical rotation of light by PO in solution, α_{sol}, the formalism above yields

$$\alpha'_D(\beta) = \frac{\alpha(\beta)}{x_{tot}\alpha_{sol}} = \left(\frac{1 + \overline{\alpha}\overline{K}_L}{1 + \overline{K}_L}\right) + \left[\left(\frac{1 + \overline{\alpha}\overline{K}_L}{1 + \overline{K}_L}\right) + \left(\frac{1 + \overline{\alpha}\overline{K}_D}{1 + \overline{K}_D}\right)\right]\beta \tag{11a}$$

for optical rotation by the solution containing D-cys/Au NPs and

$$\alpha'_L(\beta) = \frac{\alpha(\beta)}{x_{tot}\alpha_{sol}} = \left(\frac{1 + \overline{\alpha}\overline{K}_D}{1 + \overline{K}_D}\right) + \left[\left(\frac{1 + \overline{\alpha}\overline{K}_L}{1 + \overline{K}_L}\right) + \left(\frac{1 + \overline{\alpha}\overline{K}_D}{1 + \overline{K}_D}\right)\right]\beta \tag{11b}$$

for optical rotation by the solution containing L-cys/Au NPs. Here we define the quantity α' which is a scaled and dimensionless optical rotation constant. The three unknown parameters in Eqs. (11a) and (11b) are defined as follows:

$$\overline{\alpha} = \alpha_{ads}^R/\alpha_{sol}^R = \alpha_{ads}^S/\alpha_{sol}^S \tag{12}$$

$$\overline{K}_D = S_0 K_D^R = S_0 K_L^S \tag{13a}$$

$$\overline{K}_L = S_0 K_D^S = S_0 K_L^R. \tag{13b}$$

It is important to note that Eqs. (11a) and (11b) are linear in β and thus, as noted above, one cannot independently determine all three unknown parameters on the basis of measurements that vary only β, the fractional concentrations of R- and S-PO. Also note that S_0 and K are coupled as S_0K in Eqs. (11a) and (11b) and thus, cannot be determined independently from these optical rotation measurements, when performed in a low coverage limit in which the isotherms are linear.

The second experimental protocol is one in which the concentration of either R-PO or S-PO is held constant at x_{tot}. However, the fractional concentration of the D-cys/Au and L-cys/Au NPs is varied while their total concentration, represented by S_0, is kept constant. The fractional concentration of the D-cys/Au and L-cys/Au NPs as quantified by, γ, is varied from 0 to 1. For the solution containing S-PO the dependence of the optical rotation on γ is given by

$$\alpha'_S(\gamma) = \frac{1 + \overline{\alpha}(\gamma\overline{K}_L + (1-\gamma)\overline{K}_L)}{1 + (\gamma\overline{K}_L + (1-\gamma)\overline{K}_L)} \tag{14a}$$

and for the solution containing R-PO the dependence of the optical rotation on γ is given by

$$\alpha'_R(\gamma) = -\frac{1 + \overline{\alpha}(\gamma\overline{K}_D + (1-\gamma)\overline{K}_L)}{1 + (\gamma\overline{K}_D + (1-\gamma)\overline{K}_L)}. \tag{14b}$$

These equations are non-linear in γ.

One can fit optical rotation data collected as functions of β and γ to Eqs. (11a), (11b), (14a) and (14b) to estimate the values of the three parameters $\overline{\alpha}$, $\overline{K}_D$ and $\overline{K}_L$. Given that the specific optical rotation of light by R- and S-PO in solution phase can be measured easily and independently of the measurements above, parameter estimation of $\overline{\alpha}$ ultimately yields the value of $\alpha_{ads}^R = -\alpha_{ads}^S$. More importantly, parameter estimation of the values of $\overline{K}_D$ and $\overline{K}_L$ allows direct estimation of the enantiospecific ratios of the adsorption equilibrium constants, $K_D^R/K_L^R = K_L^S/K_D^S = \overline{K}_D/\overline{K}_L$ without the need to determine the value of S_0. This is a key feature of the measurement protocol and the analysis that allows robust estimation of the enantioselectivity of adsorption on chiral NPs.

3. Experimental protocol

The synthesis of the chiral Au NPs was conducted as described earlier [16]. The measurements of optical rotation were conducted using a Rudolph Analytics optical polarimeter. Each optical rotation value was determined from a set of ten optical rotation measurements made automatically by the instrument and reported as an average value and a standard deviation.

Prior to making measurements of optical rotation in solutions with varying concentrations of D- and L-cys/Au NPs and R- and S-PO, a set of measurements was conducted using a solution of L-cys/Au NPs and increasing concentrations of R-PO. These were used to determine the PO concentration range over which the optical rotation varied linearly, in order to be sure that the basic approximation of Eq. (5) holds and that the study was conducted within the linear regime of the PO/cys/Au NP adsorption isotherm. The other quantity that was measured independently was $\alpha_{sol}^R = -\alpha_{sol}^S$, obtained by measuring the optical rotations of solutions with increasing concentrations of R- or S-PO and determining the proportionality constant between optical rotation and concentration.

The principal feature of the measurement protocol developed in the course of this work was related to the preparation of the solutions. In the case of the measurements that spanned $\beta = 0 \rightarrow 1$, the fractional concentrations of R- and S-PO, two 10 ml aqueous solutions were prepared initially with identical concentrations of D-cys/Au NPs and equal concentrations of R-PO and S-PO. In this case, $x_{tot} = 0.5$ M. After measuring the optical rotation by these two solutions having $\beta = 0$ and $\beta = 1$, aliquots of 1 ml were taken from each 10 ml solution and then transferred to the other. Optical rotation measurements were then made using these solutions now having $\beta = 0.11$ and $\beta = 0.89$. Then 1 ml aliquots were transferred between the two and additional optical rotation measurements were made. Repeating in this manner the values of β for the two solutions were varied from $\beta = 0$ and $\beta = 1$ until both were arbitrarily close to $\beta = 0.5$, all the while holding the

concentration of D-cys/Au NPs constant. Once complete, the protocol was then repeated starting with two 10 ml solutions with identical concentrations of L-cys/Au NPs.

A similar protocol was used for the measurements in which the fractional concentration of D- and L-cys/Au NPs was varied from $\gamma = 0$ to 1. Note that in these measurements, the concentrations of the Au NPs in solution are determined by the synthesis conditions and need not be determined for the purposes of determining the ratio of the enantiospecific adsorption equilibrium constants. Two 10 ml solutions were initially prepared with equal concentrations of D-cys/Au and L-cys/Au NPs and identical concentrations of 0.5 M R-PO. After initial optical rotation measurements had been made on each solution, 1 ml aliquots of each were transferred between the two and optical rotation measurements were repeated on the solutions with their new values of γ. This sequence was repeated until the two solutions approached $\gamma = 0.5$, all the while maintaining the concentration of R-PO at 0.5 M. The protocol was then repeated using solutions starting with concentrations of 0.5 M S-PO, rather than R-PO.

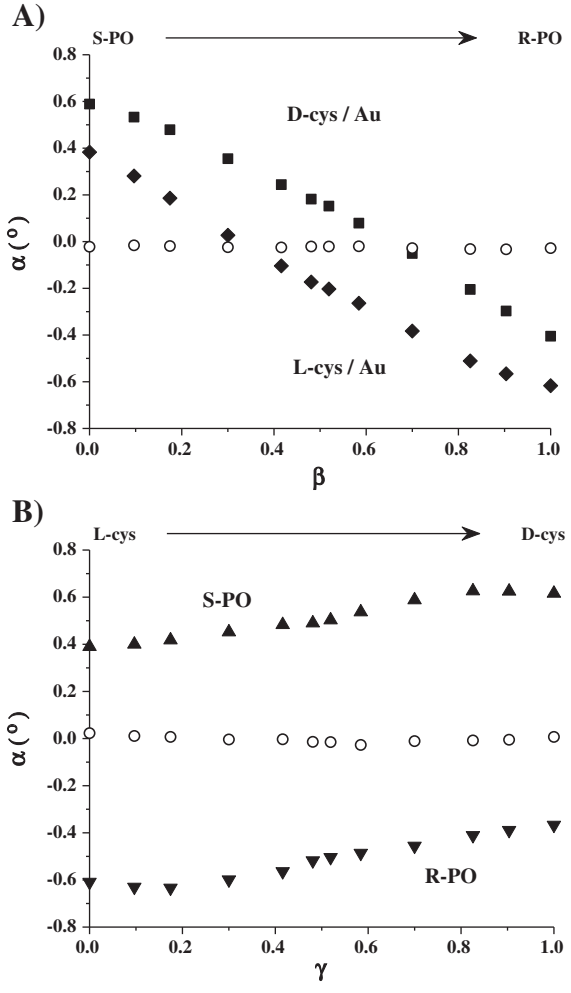

Fig. 2. A) Optical rotation angle versus β (fractional concentration of R-PO in solutions containing a total R-PO + S-PO concentration of 0.5 M). The solutions also contain either D-cys/Au (■) or L-cys/Au (♦). The open circles (○) are the sum of the optical rotations at β in the presence of L-cys/Au and at $1 - \beta$ in the presence of D-cys/Au. B) Optical rotation angle versus γ (fractional concentration of D-cys/Au NPs in solutions containing a fixed total D-cys/Au + L-cys/Au concentration). The solutions also contain either S-PO (▲) or R-PO (▼) at concentrations of 0.5 ML. The open circles (○) are the sum of the optical rotations at γ in the presence of S-PO and at $1 - \gamma$ in the presence of R-PO. The fact that the open circles (○) in both A) and B) have values of ~0 indicates that both data sets reveal diastereomerism in their optical rotations.

4. Results and discussion

The optical rotations of four sets of solutions containing R- and S-PO and D- and L-cys/Au NPs have been obtained as described above. The total concentration of PO in solution was held at 0.5 ML. This concentration was within the linear range of the optical rotation measurements and, therefore, the linear range of the adsorption isotherms. Note also that the optical rotations due just to the D-cys/Au and L-cys/Au NPs were measured and then subtracted from the values resulting from the addition of the R- and S-PO.

The first set of measurements varied the quantity β, the fractional concentration of R-PO while holding the concentrations of D-cys/Au or L-cys/Au fixed. The optical rotation angles for each of the two sets of solutions, $\alpha_D(\beta)$ and $\alpha_L(\beta)$, are plotted in Fig. 2A. Note that as predicted by Eqs. (11a) and (11b), the optical rotations are roughly linear in β. The open circles plotted in Fig. 2A are the sums $\alpha L(\beta) + \alpha D(1 - \beta)$, all of which have magnitudes close to zero. The offset between $\alpha_D(\beta)$ and $\alpha_L(\beta)$ and the diastereomeric relationship between the two demonstrates the enantiospecific adsorption of R- and S-PO on the D-cys/Au or L-cys/Au NPs.

The second set of measurements varied the quantity γ, the fractional concentration of D-cys/Au, while holding the concentrations of R-PO or S-PO fixed at 0.5 M. The optical rotation angles for each of the two sets of solutions, $\alpha_R(\gamma)$ and $\alpha_S(\gamma)$, are plotted in Fig. 2B. The open circles plotted in Fig. 2B are the sums $\alpha S(\gamma) + \alpha R(1 - \gamma)$. As in Fig. 2A, these are almost zero. The diastereomeric relationship between $\alpha_R(\gamma)$ and $\alpha_S(\gamma)$ demonstrates the enantiospecific adsorption of R- and S-PO on the D-cys/Au or L-cys/Au NPs.

Analysis of the data in Fig. 2 has been performed by scaling the optical rotations by $x_{tot} = 0.5$ M and by $\alpha_{sol} = 0.72°$ as indicated in Eqs. (11a) and (11b) to yield the dimensionless quantities $\alpha'_D(\beta)$, $\alpha'_L(\beta)$, $\alpha'_R(\gamma)$ and $\alpha'_S(\gamma)$ which are plotted in Fig. 3. These have then been fit to Eqs. (11a), (11b), (14a), and (14b) to obtain estimates of the parameters $\overline{\alpha} = 6.2$, $\overline{K}_D = 0$ and $\overline{K}_L = 0.18$ defined in Eqs. (12), (13a) and (13b). The key result is that the enantiospecific adsorption equilibrium constants have magnitudes such that $K_L^R = K_D^S \gg K_D^R = K_L^S$. The fact that $\overline{K}_D = 0$ means that the adsorption of R-PO on D-cys/Au NPs or of S-PO on L-cys/Au NPs is sufficiently low that it is not detectable in these experiments.

The analysis methodology and the measurement protocol proposed in this work should be more robust than those discussed in our original observation of enantiospecific adsorption of R- and S-PO on D- and L-cys/Au NPs in that they obviate the need to use the optical rotation

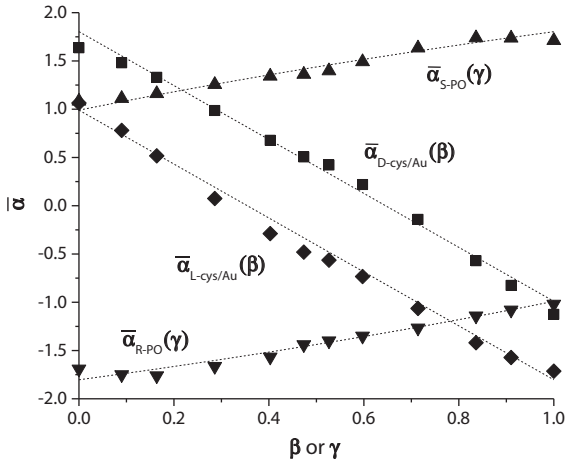

Fig. 3. Plot of the unitless optical rotation, α', versus the fractional concentrations of R-PO, β, or D-cys/Au, γ, in the four solutions for which optical rotation has been measured as illustrated in Fig. 2. The symbols are the scaled and unitless values of α' as measured, while the dashed lines are the fits of Eqs. (11a), (11b), (14a) and (14b) used to estimate the parameters $\overline{\alpha}$, $\overline{K}_D$ and $\overline{K}_L$.

data to estimate the concentration of PO adsorption sites in solution, S_0 [16]. Furthermore, it obtains estimates of $K_D^R/K_L^R = K_L^S/K_D^S = \overline{K}_D/\overline{K}_L$ across a range of coverages of adsorbed R- and S-PO rather than just one coverage, as determined by one concentration of PO in solution. The application of the method does require further investigation of the sensitivity of the estimated parameters to experimental variables such as PO concentration. In addition, it requires further study of some of the underlying assumptions, such as the use of a simple linear isotherm in the low coverage limit. This assumption ignores the potential for interactions between enantiomers that might result in the formation of conglomerate (R–R, S–S) or racemate (R–S) phases of adsorbed PO and might require description using more sophisticated isotherms.

5. Conclusions

The measurement of optical rotation by solutions containing various relative concentrations of R- and S-PO mixed with D-cys/Au and L-cys/Au NPs has been used to demonstrate the enantiospecific interactions of the R- and S-PO with the chirally modified Au NPs. This has been demonstrated across a wide range of enantiomeric excess of the PO in solution. In addition, an initial attempt has used a simple adsorption model to extract quantitative estimates of the ratios of the adsorption equilibrium constants, $K_D^R/K_L^R = K_L^S/K_D^S$, from the optical rotation measurements. The show that $K_L^R = K_D^S \gg K_D^R = K_L^S$.

Acknowledgments

AJG and NS acknowledge the support from the DOE grant DE-FG02-03ER15472. NO acknowledges the support from a CMU SURG grant.

References

[1] I. Lee, F. Delbecq, R. Morales, M.A. Albiter, F. Zaera, Nat. Mater. 8 (2009) 132.
[2] P.D. Jadzinsky, G. Calero, C.J. Ackerson, D.A. Bushnell, R.D. Kornberg, Science 318 (2007) 430.
[3] C. Gautier, T. Burgi, ChemPhysChem 10 (2009) 483.
[4] C. Noguez, I.L. Garzon, Chem. Soc. Rev. 38 (2009) 757.
[5] H. Yao, Curr. Nanosci. 4 (2008) 92.
[6] D.S. Sholl, A.J. Gellman, AIChE J 55 (2009) 2484.
[7] Y. Yun, A.J. Gellman, Angew. Chem. Int. Ed. 52 (2013) 3394.
[8] Z.J. An, M. Yamaguchi, Chem. Commun. 48 (2012) 7383.
[9] B.K. Canfield, S. Kujala, K. Laiho, K. Jefimovs, T. Vallius, J. Turunen, M. Kauranen, J. Nonlinear Opt. Phys. Mater. 15 (2006) 43.
[10] C.L. Chang, X. Wang, Y. Bai, H.W. Liu, Trends Anal. Chem. 39 (2012) 195.
[11] I. Dolamic, S. Knoppe, A. Dass, T. Burgi, Nat. Commun. (2012) 3.
[12] C. Gautier, T. Buergi, Chimia 62 (2008) 465.
[13] M.W. Heaven, A. Dass, P.S. White, K.M. Holt, R.W. Murray, J. Am. Chem. Soc. 130 (2008) 3754.
[14] N. Hendler, L. Fadeev, E.D. Mentovich, B. Belgorodsky, M. Gozin, S. Richter, Chem. Commun. 47 (2011) 7419.
[15] V.I. Sokolov, Russ. J. Coord. Chem. 35 (2009) 553.
[16] N. Shukla, M.A. Bartel, A.J. Gellman, J. Am. Chem. Soc. 132 (2010) 8575.
[17] J.D. Horvath, L. Baker, A.J. Gellman, J. Phys. Chem. C 112 (2008) 7637.
[18] J.D. Horvath, A.J. Gellman, J. Am. Chem. Soc. 123 (2001) 7953.
[19] C.F. McFadden, P.S. Cremer, A.J. Gellman, Langmuir 12 (1996) 2483.
[20] X.Y. Zhao, S.S. Perry, J.D. Horvath, A.J. Gellman, Surf. Sci. 563 (2004) 217.
[21] B.S. Mhatre, V. Pushkarev, B. Holsclaw, T.J. Lawton, E.C.H. Sykes, A.J. Gellman, J. Phys. Chem. C 117 (2013) 7577.
[22] T.J. Lawton, V. Pushkarev, D. Wei, F.R. Lucci, D.S. Sholl, A.J. Gellman, E.C.H. Sykes, J. Phys. Chem. C 117 (2013) 22290.